Applied Problems of Nonlinear Oscillation and Wave Theory

Izvestiya Vysshikh Uchebnykh Zavedeniy. Applied Nonlinear Dynamics. 2023;31(2)

Article DOI: 10.18500/0869-6632-003030

Mechanisms leading to bursting oscillations in the system of predator–prey communities coupled by migrations

E. V. Kurilova, M. P. Kulakov✉*, E. Ya. Frisman*

Institute for Complex Analysis of Regional Problems,
Far Eastern Branch, Russian Academy of Sciences, Birobidzhan, Russia
E-mail: katkurilova@mail.ru, ✉k_matvey@mail.ru, frisman@mail.ru
Received 22.09.2022, accepted 26.12.2022, available online 27.02.2023, published 31.03.2023

Abstract. The *purpose* is to study the periodic regimes of the dynamics for two non-identical predator–prey communities coupled by migrations, associated with the partial synchronization of fluctuations in the abundance of communities. The combination of fluctuations in neighboring sites leads to the regimes that include both fast bursts (bursting oscillations) and slow oscillations (tonic spiking). These types of activity are characterized by a different ratio of synchronous and non-synchronous dynamics of communities in certain periods of time. In this paper, we describe scenarios of the transition between different types of burst activity. These types of dynamics differ from each other not so much in size, shape, and number of spikes in a burst, but in the order of these bursts relative to the slow-fast cycle. *Methods.* To study the proposed model, we use the bifurcation analysis methods of dynamic systems, as well as geometric methods based on the division of the full system into fast and slow equations (subsystems). *Results.* We showed that the dynamics of the first subsystem with a slow-fast limit cycle directly determines the dynamics of the second one with burst activity through a smooth dependence of regime on the number of predators and a non-smooth dependence on the number of prey. We constructed the invariant manifolds on which there are parts of dynamics with tonic (slow manifold) and burst (fast manifold) activity of the full system. *Conclusion.* We described the scenario for bursting with different waveforms, which are determined by the appearance of the fast invariant manifold and the location of its parts relative to the slow-fast cycle. The transitions between different types of burst are accompanied by a change in the oscillation period, the degree of synchronization, and, as a result, the dynamics becomes quasi-periodic when both communities are not synchronous with each other.

Keywords: predator–prey, migration, synchronization, tonic spiking, bursting, slow-fast system.

Acknowledgements. This work was carried out within the framework of the state targets of the Institute for Complex Analysis of Regional Problem of the Far Eastern Branch of the Russian Academy of Sciences.

For citation: Kurilova EV, Kulakov MP, Frisman EYa. Mechanisms leading to bursting oscillations in the system of predator–prey communities coupled by migrations. Izvestiya VUZ. Applied Nonlinear Dynamics. 2023;31(2):143–169. DOI: 10.18500/0869-6632-003030

Introduction

The study of population biology models for a long time continues to be one of the actively developing areas of world and domestic science. Works devoted to the study of the dynamics of the development of biological systems functioning on the principle of predator-prey, parasite-host, resource-consumer, etc., are becoming increasingly in demand. [1]. The popularity of these studies is based on the constant expansion of the scope of their application, which contributes to obtaining new, increasingly complex and interesting results, despite, and possibly due to the rich history of research and significant elaboration of the corresponding mathematical apparatus. Thus, the pandemics hanging over humanity lead to the relevance and put at the peak of popularity the research of ecological and epidemiological models describing the spread of infections in populations based on the interaction of healthy and infected individuals functioning on the principle of predator-prey or parasite-host [2, 3].

The study of dynamic models of biological systems, regardless of their field of application, is based, as a rule, on the apparatus of ordinary differential equations. When studying models of several interacting communities, nonlinear phenomena that occur during synchronization of dynamics in different territories are of particular interest [4–6] and related, for example, to the mechanisms of formation of spatio-temporal heterogeneity, complex dynamic behavior, etc. [7–12].

One of the most popular areas of nonlinear dynamics is the study of neural activity, which is described by fast-slow systems. In such systems, so-called explosive oscillations often occur [13–16]. Over the past decades, various types of such oscillations have been discovered and described, as well as the bifurcation mechanisms leading to them have been studied in detail [17–21].

This work is one of such studies and is devoted to the study of the population dynamics of two adjacent non-identical migrationally related communities, each of which is an auto-oscillatory subsystem and functions according to the principle of «predator-prey» with a Holling type II functional response [22, 23]. The system under consideration is a modification of the Bazykin equations [24, 25] — one of the basic models of population biology, referred to in foreign literature as the model Rosenzweig–MacArthur [26, 27].

Our earlier study of the synchronization of regular oscillations occurring in the system under consideration revealed several features [28–30]. Firstly, in the case of a strong connection, complete synchronization of cycles in different territories is possible, even with a significant difference between communities [29]. However, this leads to the only possible type of dynamics — the limit cycle. Secondly, a decrease in the strength of the connection leads to a very rapid desynchronization, in which each community experiences fluctuations in numbers with their own rhythm. As a result, in the case of weak communication, synchronization is possible only for identical communities, and communities that differ little are unable to fully synchronize. In general, the listed results are in good agreement with the results of other authors. However, further research has shown that loosely connected non-identical communities are capable of at least partial synchronization precisely in the case of a large difference between the values of predator mortality [28]. In addition, as a result of the study, modes were found that combine both areas with rapid explosive fluctuations (burst activity) and tonic spiking. The emergence of such modes occurs when the differences between the communities under consideration change as a result of their partial synchronization. This leads to the formation of a complex phase trajectory combining sections of synchronous and non-synchronous dynamics at different time intervals. The degree of synchronization significantly affects the change in the pattern of dynamic behavior, which in turn affects the change in the type of bursting activity [30].

In this paper, in addition to generalizing the results obtained earlier, based on the technique of dividing the complete system into slow and fast subsystems, a detailed study and description of scenarios for the formation of different types of burst activity affecting the change in the shape of the burst is carried out.

1. A model of the dynamics of two non-identical communities coupled by migration

The equations of population dynamics of two neighboring non-identical migrationally related «predator-prey» communities described by the Bazykin equations [24, 25] with a Holling type II functional response, have the form:

$$\begin{cases} \dfrac{dX_1}{dt} = A_1 X_1 \dfrac{K - X_1}{K} - \dfrac{BX_1Y_1}{1 + HX_1}, \\ \dfrac{dY_1}{dt} = -CY_1 + \dfrac{SX_1Y_1}{1 + AX_1} + M\left(Y_2 - Y_1\right), \\ \dfrac{dX_2}{dt} = A_2 X_2 \dfrac{K - X_2}{K} - \dfrac{BX_2Y_2}{1 + HX_2}, \\ \dfrac{dY_2}{dt} = -CY_2 + \dfrac{SX_2Y_2}{1 + HX_2} + M\left(Y_1 - Y_2\right), \end{cases} \tag{1}$$

where X_1 and X_2 — the number of prey populations, Y_1 and Y_2 — the number of predator populations in the first and second communities, respectively; K — stable equilibrium number of prey populations in each habitat in the absence of a predator; B — specific rate of consumption by the predator population of the prey population at a unit density of both populations; C — natural mortality of the predator; S/B — coefficient of processing the prey biomass consumed by the predator into its own biomass; H — the predator handling time; M — predator migration coefficient. The non-identity of the communities is expressed in a significant difference in the maximum reproduction rates of the prey populations, designated as A_1 and A_2, respectively ($A_1 \neq A_2$). This reflects the situation when two fundamentally different types of preys live in adjacent territories, but having the same food value for a predator.

After replacing the variables: $X_i = Cx_i/s$, $Y_i = A_i y_i/b$ $(i = 1, 2)$, the model (1) is converted to the following system with five parameters:

$$\begin{cases} \dfrac{dx_1}{dt} = x_1(1 - ax_1) - \dfrac{x_1y_1}{1 + hx_1}, \\ \dfrac{dy_1}{dt} = -c_1y_1 + \dfrac{c_1x_1y_1}{1 + hx_1} + c_1m\left(\dfrac{c_1}{c_2}y_2 - y_1\right), \\ \dfrac{dx_2}{dt} = x_2(1 - ax_2) - \dfrac{x_2y_2}{1 + hx_2}, \\ \dfrac{dy_2}{dt} = -c_2y_2 + \dfrac{c_2x_2y_2}{1 + hx_2} + c_2m\left(\dfrac{c_2}{c_1}y_1 - y_2\right), \end{cases} \tag{2}$$

where x_i and y_i are the relative numbers of prey and predator, $h = HC/S$ — the predator handling time, $a = C/(KS)$ — prey self-imitation coefficient, $c_i = C/A_i$ — relative rate of decline (loss) of predator numbers (mortality) and $mc_i = M/A_i$ — predator migration coefficient $(i = 1, 2)$. The article [28] describes the problem statement in more detail and provides an analytical study of the system (1).

It should be noted that the substitution of variables used in the system (2) leads to the fact that two non-identical communities with different birth rate of preys ($A_1 \neq A_2$) become similar to

communities in which the mortality of predators is different ($c_1 \neq c_2$). However, in this case, the relationship between communities are asymmetric ($c_1 m \neq c_2 m$), that is, the rates of outflow of individuals leaving one territory (emigrants) and the rates of their influx to another (immigrants) do not coincide, which can be interpreted as the death of predators during migration. However, due to the difference in mortality of the predator ($c_1 \neq c_2$), this death will be different when moving from the first or second community, which directly indicates the most «advantageous» direction for emigration: the territory where the mortality of the predator or the birth rate of preys is higher, which is equivalent, according to the variable substitution used.

For further investigation of the dynamics modes arising in the communities, we will take the following parameter values:

$$a = 0.1, \quad h = 0.5, \quad c_1 = 0.002, \quad c_2 = 0.5, \quad m = 0.005,$$

where the values a, h give rise to a limit cycle in each of the subsystems corresponding to different communities. The value of $c_1 = 0.002$ corresponds to the low mortality of predators in the first territory, and $c_2 = 0.5$ — high mortality of predators on the second. According to the above substitution of variables from (1) to (2), a community with low predator mortality has a high rate of reproduction of prey, and vice versa, high predator mortality is inherent in a community with a slow rate of growth in the number of prey. Such a situation is possible when the habitats of preys haves fundamentally different reproductive potential. For example, the preys are rapidly reproducing small rodents and slowly reproducing large herbivores that live in different territories (meadow and forest), and the predator moves between them.

In the course of the study, we will vary a and c_1 at fixed $h = 0.5$, $c_2 = 0.5$, $m = 0.005$, monitoring the stability of equilibrium points and studying the type of dynamic behavior.

Analytical research has shown that the system (2) has several equilibriums:

- trivial $A_0(0;0;0;0)$ with zero numbers of all populations;
- semi-trivial $A_1(1/a;0;0;0)$, $A_2(0;0;1/a;0)$, $A_3(1/a;0;1/a;0)$ with zero predators;
- semi-trivial $B_1\Big(\dfrac{1+2m}{\beta_1};\dfrac{(1+m)\beta_2}{\beta_1^2};0;\dfrac{c_2 m\beta_2}{c_1\beta_1^2}\Big)$ and $B_2\Big(0;\dfrac{c_1 m\beta_2}{c_2\beta_1^2};\dfrac{1+2m}{\beta_1};\dfrac{(1+m)\beta_2}{c_1\beta_1^2}\Big)$ ($\beta_1 = 1-h+m-2hm$, $\beta_2 = \beta_1 - a - 2am$) corresponding to zero numbers of one prey population in different communities;
- three nontrivial $E_i\Big(\bar{x}_1^{(i)},\bar{y}_1^{(i)},\bar{x}_2^{(i)},\bar{y}_2^{(i)}\Big)$ $(i = 0,1,2)$ with non-zero numbers of all populations.

The coordinates of all points were calculated, the conditions of their existence were investigated and the simplest bifurcations were described [28, 30]. The construction of bifurcation diagrams was carried out using the open system for the study of dynamic systems MatCont [31], as well as its own set of programs. To isolate the area of quasi–periodic dynamics, the Lyapunov exponent maps method was used, as well as the method of dynamic mode maps constructed for the corresponding Poincaré mapping. The result of this study is summarized in Fig. 1.

In Fig. 1, *a* lines mark the main local bifurcations of equilibrium points of the system (1), and several areas corresponding to different types of dynamics are highlighted in color. The line TC corresponds to the transcritical bifurcation between the points B_1 and E_1. Between the lines H and H^- there is a region of existence of asymptotically stable limit cycles (the white region) arising around the equilibrium points marked in parentheses. When crossing the line H^- cycles lose stability and relaxation limit cycles are formed, also known as fast-slow cycle, or canard [21, 32–34]. In Fig. 1, *d*–*e* shows examples of the transition of limit values cycles L_1 and L_2 in fast-slow cycles C_1 and C_2, which differ greatly in the increased range of oscillations, as well as the structure shown in the second column. The phase portraits show that, in contrast

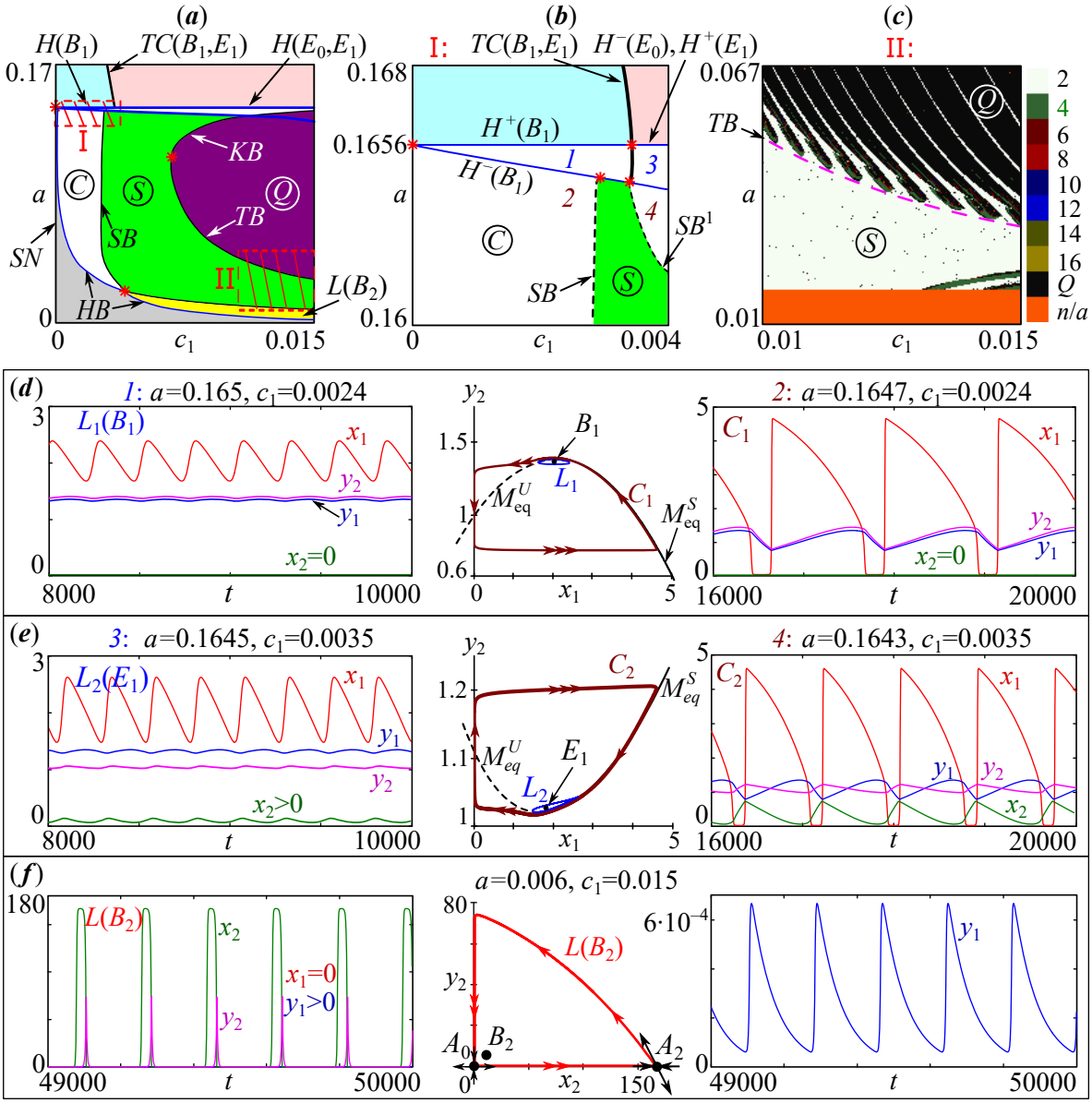

Fig. 1. *a* — Bifurcation diagram of the system (2) and *b* — its enlarged fragment. Point B_1 or E_1 is stable above the line H. The gray domain is the absence of oscillations (the point A_0 is asymptotically stable); white domain C is the region of stable limit cycles; green domain S corresponds to burst dynamics; magenta domain Q is quasi-periodic dynamics. Lines H, TC and HB are Andronov–Hopf, transcritical and homoclinic bifurcations respectively; SB is the birth of burst dynamics; KB and TB are the emergence of quasi-periodic dynamics. *c* — map of dynamic regimes in region II where color coded is the cycle period of the Poincaré mapping. *d–f* — examples of limit cycles in system (2) (color online)

to the limit cycles, L_1 and L_2, cycles C_1 and C_2 «stick» to the marked branch of the parabola (M^S_{eq}) and one of the coordinate axes (Oy_2), and also contain sections with fast (two or more arrows) and slow (one arrow) movement phase points.

When approaching the line HB, relaxation cycles increase their scope, the oscillation period increases indefinitely and the maximum canard is formed. At the intersection of this line, the cycle merges with the homoclinic loop, originating from the point A_1 or A_2 (depending on the value of c_1), and quickly collapses. As a result, there are no fluctuations in the gray area with small values of the parameter a, and the number of all communities is slowly falling. With parameter values from the narrow yellow area in Fig. 1, a a long-period cycle is formed $L(B_2)$ around the semi-trivial point B_2. An example of such a cycle is shown in Fig. 1, *f*. This cycle is characterized by a zero number of prey in the first territory ($x_1 = 0$), as well as strong and short bursts of numbers after long periods of their extremely low values. Shown in Fig. 1, f the cycle is close to its maximum size and the phase portrait shows that it passes in the vicinity of the saddle point A_2, and with a small disturbance merges with the separatrix of the point A_2 and quickly collapses.

In the green area — the S area in Fig. 1, a — a relaxation cycle is implemented, as well as multi-frequency periodic modes (Fig. 2), combining both slow tonic changes in numbers and fast burst activity. These modes on population dynamics graphs have diamond-shaped, triangular (Fig. 2, a), truncated trapezoidal (Fig. 2, b) or more complex shapes (Fig. 2, c), and differ in the number of turns on the fast burst diversity. The number of turns increases as we approach the area quasi-periodic dynamics Q (fig. 2, d–f).

In the magenta area Q (see Fig. 1, a) the model trajectory tightly covers such sets as the torus (at the intersection of the line TB) (see Fig. 2, f) or the Klein bottle (lines KB) (see

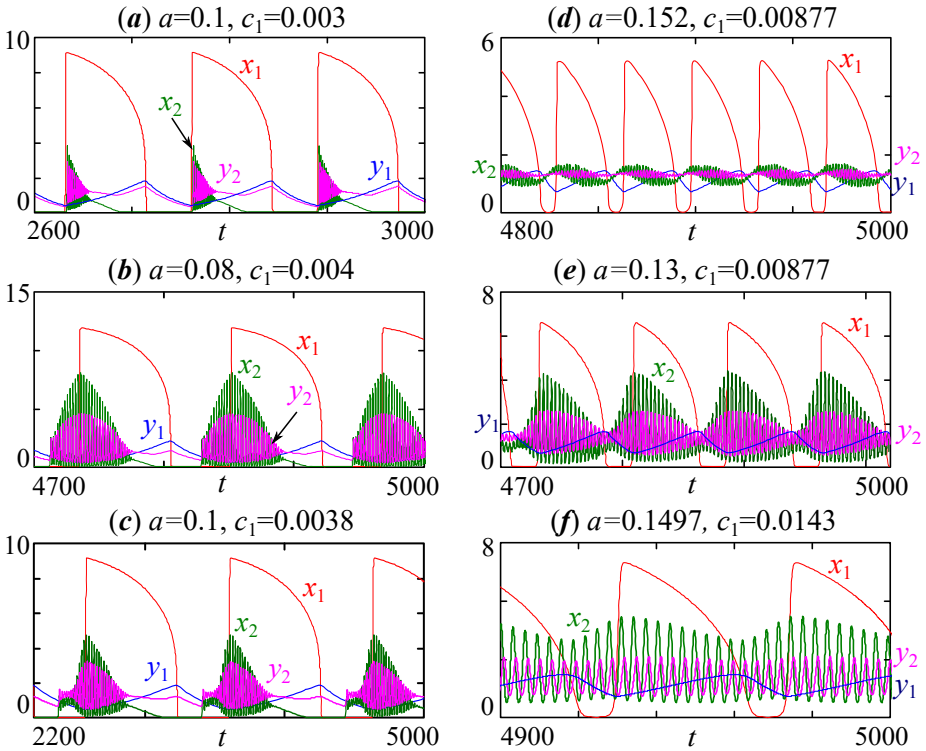

Fig. 2. Examples of bursting in system (2) from region S (fig. 1) which differ in the waveform of burst (color online)

fig. 2, *d*, *e*), and periods of fluctuation of communities in different territories are connected by an irrational ratio. This type of dynamics was previously considered through analysis of Poincare mapping, [30]. In this case, the trajectory forms closed invariant curves on a specially selected cutting plane, which, in the case of dynamics on a torus or a Klein bottle, have different mutual positions. It is found that in the first case the curves are nested into each other, and in the second — are located far enough from each other.

Further, as c_1 grows, only a quasi-periodic type of dynamics is observed, and only at $c_1 \to c_2$ complete synchronization occurs. Chaotic modes at the accepted parameter values were not detected in this model.

Based on numerical experiments, it can be argued that the regions of S and Q (see Fig. 1, *a*) are heterogeneous. In the first area, there is an alternation of modes that differ in the order of the fast burst part of the cycle relative to the slow one. In the area of Q the region of quasi-periodic dynamics (in Fig. 1, *c* marked in black) alternate with synchronization tongues (coded by color) — areas of parameters leading to strictly periodic dynamics. The number on the map dynamic modes (see fig. 1, *c*) indicates the number of full cycle revolutions required to return the model trajectory to the starting point of the phase space. Outside of tongues, this number is infinitely large.

The rates of change of the variables y_1 and y_2 are determined by the parameters c_1 and c_2, taking into account the selected parameter values $0 < c_1 \ll c_2 < 1$, therefore, we can assume that $0 < c_1 \ll 1$ — small parameter. This allows us to consider this model as a fast-slow system. In the sense that the first two equations constitute a slow subsystem in which only a slow cycle is observed, and the last two are fast, in which fluctuations with a period much longer than that of the slow subsystem are possible. Let's use the methodology of studying fast-slow systems to study the system (2).

In the study of such dynamical systems, geometric methods are often used based on the separation of the complete system (2) into fast and slow equations (subsystems). In this case, the variation of the slow variable, which is a bifurcation or scanning parameter, in the extreme case, makes it possible to simplify the search for bifurcations of equilibrium states leading to the birth of limit cycles of a fast (two-dimensional) subsystem considered in the limit $c_1 = 0$. Also, changing the scanning parameter for small $c_1 \neq 0$ makes it possible to construct a slow critical manifold, being a skeleton for various types of activities in a complete fast-slow model (2). It is obvious that the fast subsystem of the model (2) has at least two such manifolds: a rest manifold and a spiking manifold on which fast bursts of numbers occur (spikes) shown in Fig. 2. Moreover, the synergy of fast and slow interactions can lead to very atypical bifurcation phenomena, possible only in the full model [17, 35, 36].

Further, in accordance with the geometric method, we investigate the bifurcations arising in each of the subsystems and compare them with the modes of the complete system.

2. Bifurcations in the slow and fast subsystem

Consider subsystems, each of which corresponds to a local community independently of each other. For a deeper study of the processes occurring in the first community, we will assume that the number of prey and predators of the second community changes quite slowly and has little effect on the dynamics of the first. In this case, the model (2) is transformed into a system of the form:

$$\begin{cases} \dfrac{dx_1}{dt} = x_1(1 - ax_1) - \dfrac{x_1 y_1}{1 + hx_1} = f_1(x_1, y_1), \\ \dfrac{dy_1}{dt} = c_1 \left(-y_1(1 + m) + \dfrac{x_1 y_1}{1 + hx_1} + \dfrac{c_1 m}{c_2} y_2 \right) = c_1 g_1(x_1, y_1, y_2), \\ \dfrac{dx_2}{dt} = \dfrac{dy_2}{dt} = 0. \end{cases} \tag{3}$$

In the system (3) there is a small parameter c_1 ($0 < c_1 \ll c_2 < 1$), which enters the second equation twice. The presence of a small c_1 leads to, that the influence of the «frozen» variable y_2 on the system is much weaker than y_1 and x_1.

For the second subsystem, similarly, we can write:

$$\begin{cases} \dfrac{dx_1}{dt} = \dfrac{dy_1}{dt} = 0, \\ \dfrac{dx_2}{dt} = x_2(1 - ax_2) - \dfrac{x_2 y_2}{1 + hx_2} = f_2(x_2, y_2), \\ \dfrac{dy_2}{dt} = -c_2 y_2 + \dfrac{c_2 x_2 y_2}{1 + hx_2} + c_2 m \left(\dfrac{c_2}{c_1} y_1 - y_2 \right) = g_2(x_2, y_2, y_1). \end{cases} \tag{4}$$

The system (4) significantly depends on the parameter y_1, because $c_2^2 m / c_1 \gg c_1$.

Let's call the system (3) leading or strong, and (4) — driven or weak. We show that a strong system (3) determines the dynamics (4), as well as the joint dynamics of the complete system (2).

To begin with, let's consider bifurcations in the subsystem (3) when changing the parameter y_2. The equilibrium states of this subsystem lie in the plane (x_1, y_1), at the intersection of two nullcline $f_1(x_1, y_1) = 0$ and $g_1(x_1, y_1, y_2) = 0$, where y_2 is parameter.

As is known [17, 33], for systems of the form (3) in the limiting case $c_1 = 0$ equation $f_1(x_1, y_1) = 0$ sets a critical manifold in the phase space or slow curve: $M_{eq} = \left\{ (x_1, y_1) \in R^2 \middle| f_1(x_1, y_1) = 0 \right\} \cup \{x_1 = 0, y_1 \geqslant 1\}$. Note that it becomes a surface for the complete system (2). This piecewise curve contains a stable M_{eq}^S (the upper part of the parabola in Fig. 3, *a*) and unstable M_{eq}^U branches (lower part of the parabola and part of the line $x_1 = 0$). In Fig. 3, *a* these branches are shown by solid and dotted lines, and act as the basis of the relaxation cycle in the leading system (3) at sufficiently small $c_1 \neq 0$. As shown in Fig. 3, *a* one part of the cycle lies on a stable branch of the manifold M_{eq}^S, other on M_{eq}^U.

The point $\langle \mathbf{z} \rangle$ in Fig. 3, *a* and fig. 5 corresponds to the center «mass» of the limit cycle (the average value of the coordinates) and is found from the standard formula [36]:

$$\langle \mathbf{z} \rangle = \frac{1}{T} \int_0^T \phi(t) dt,$$

where $\mathbf{z} = \phi(t)$ is an equation describing the change in the coordinates of the limit cycle with a period of T. For the system (3) $\mathbf{z} = (x_1, y_1)$, for (4) $\mathbf{z} = (x_2, y_2)$. When calculating this integral, the numerically obtained coordinates of the points of the limit cycle on one turn are considered, their coordinates are summed, and the result is divided by the number of points lying on cycle.

Fig. 3, *a* shows a canard that occurs in the system (3) with a fixed value of the «frozen» variable y_2. Moreover, this cycle is accurate to small order $O(c_1)$ coincides with the periodic solution of the complete system (2) at the specified parameter values. The number of arrows in Fig. 3, *a* indicates the speed of movement along canard in such a way that in the horizontal direction the cycle contains slow movement, and in the vertical direction — fast.

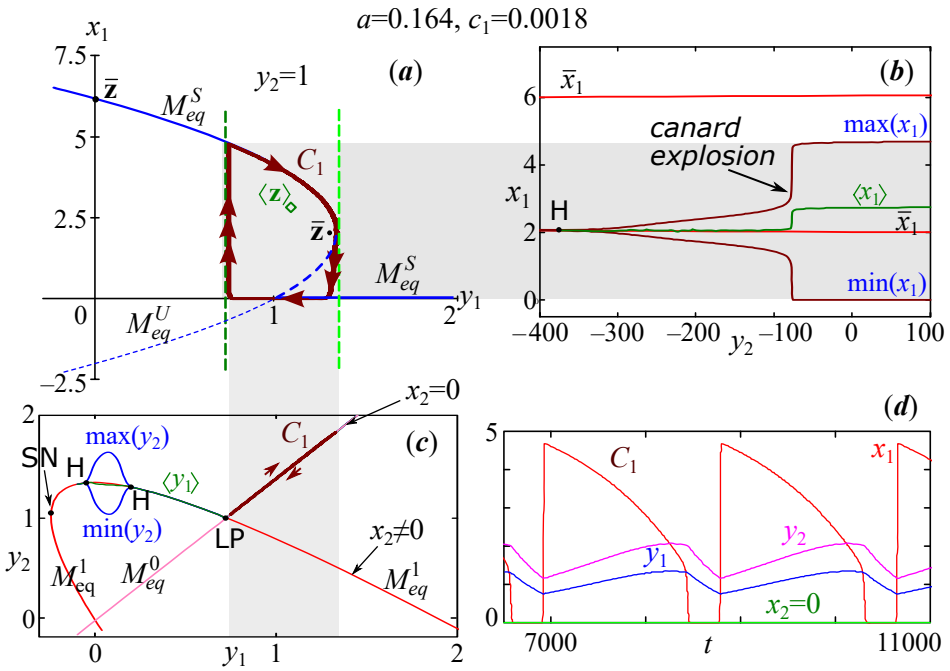

Fig. 3. *a* — Nullcline of system (3) with a slow-fast limit cycle of system (2) (canard C_1) lying on top of nullcline. *b* and *c* — Bifurcation diagram of system (3) and (4) with variation of the parameter y_2 and y_1, respectively. The gray bars highlight the range of the limit cycle C_1 falling into different parts of the diagram *b* and *c*. *d* — Dynamics of the full system (2) corresponding to cycle C_1 (color online)

For a small $c_1 \neq 0$, the variation of the parameter y_2 moves the second nullcline defined by the equation $g_1(x_1, y_1, y_2) = 0$, relative to the equilibrium point, independent of the values of y_2. Along with it, the equilibrium shifts. When $c_1 = 0$ the nontrivial point $\bar{z} = (\bar{x}_1, \bar{y}_1)$ coincides with the vertex of the parabola $f_1(x_1, y_1) = 0$, and when $c_1 > 0$ it is shifted inside the loop. Fig. 3, *b* shows the dependence of the coordinates $(\bar{x}_1)$ of the equilibriums of the system (3) on y_2. At a certain value of y_2, a bifurcation occurs in the system (3) Andronov–Hopf (point H), and a stable limit cycle is born from a stationary point. With the growth of the parameter, it increases its size (the amplitude of the oscillations). To show this, in Fig. 3, *b* shows the dependence of the extreme values of the number of prey ($\max(x_1)$ and $\min(x_1)$) of the slow subsystem (3), as well as the average value of the coordinates of the cycle $\langle x_1 \rangle$ when changing y_2. At the point designated as «canard explosion», the cycle rapidly increases in size and «sticks» (tends) to the corresponding branches of the slow curve are M_{eq}, and the center of the cycle moves significantly away from the stationary point. As a result, the phase portrait of the subsystem (3) with acceptable values $y_2 > 0$ represents a canard that practically does not change even with significant variations of the «frozen» variable y_2.

Unlike a strong community (3), a weak community (4) significantly depends on the parameter y_1. Consider the local bifurcations of the system (4) depending on y_1. The coordinates of the stationary points $\bar{x}_2$ and $\bar{y}_2$ are easy to calculate as the solution of the system

$$\begin{cases} f_2(\bar{x}_2, \bar{y}_2) = 0, \\ g_2(\bar{x}_2, \bar{y}_2, y_1) = 0. \end{cases}$$

Fig. 3, *c* shows the dependence of stationary points on the parameter y_1. This dependence is represented by the line $M^0_{eq} = \{(y_1, y_2) \in R^2 | y_2 = c_2 m y_1/(c_1(1+m)), x_2 = 0\}$ and the curve $M^1_{eq} = \{(y_1, y_2) \in R^2 | (c_2 m h y_1 - c_1((1+m)h-1)y_2)^2 - c_1 c_2 m(a+h)y_1 + c_1^2((1+m)(1+h)-1), y_2 =$

$0, x_2 > 0\}$. They intersect at the point LP, corresponding transcritical bifurcation, in which the coordinates of the stationary points coincide and stability is exchanged. To the right of it, the points are stable, located on a straight line, but with zero stationary number of prey of a weak community ($\bar{x}_2 = 0$). On the left, points on a parabola with a nonzero stationary number of prey are stable ($\bar{x}_2 > 0$). At the second intersection point, only the numbers of the predator coincide, but not the prey. Therefore, there are no qualitative changes there. We show that the sets M^0_{eq} and M^1_{eq}, as well as M_{eq}, can be considered as an approximation of a part of invariant manifolds of the complete system (2).

From the constructed bifurcation diagrams, it is easy to understand that periodic changes in the parameter y_1 caused by the fast-slow cycle (canard) in the leading system (3) provoke fluctuations in the variable y_2 in the driven system (4). As a result, the dynamics of the complete system (2) is significantly determined by where the fluctuations of y_1 fall on this chart. There are several possible options for the location of the variation y_1 in this diagram, corresponding to fundamentally different modes of the system (2).

First, if the variation y_1 lies to the right of the LP point, then the dynamics of the phase variable y_2 strictly follows all changes y_1 (see Fig. 3, *c*). As already shown, the leading system can generate only periodic fluctuations, so the dynamics of predator numbers in both areas is in-phase (see Fig. 3, *d*). The number of prey of x_2 in the driven system turns out to be zero in the asymptotic case. This limit a cycle (canard C_1) is formed around a semi-trivial stationary point B_1. In Fig. 3, *a* it is shown that when projected onto a plane (x_1, y_1) the cycle tends to the branches of the manifold M_{eq}, and when projected onto the plane (y_1, y_2) — lies on the section of the line M^0_{eq} (see Fig. 3, *c*).

Secondly, the parameter y_1 can change so that the phase points are located to the left of the LP point on the diagram. In this case, the cycle in the leading system provokes anti-phase fluctuations in the driven system with a non-zero number of prey x_2. An example of such dynamics is shown in Fig. 4, *a*, where the attractor of the complete system (2) lies only on the section of the parabola M^1_{eq}. The right shows how the values of the phase variables y_1 and y_2 change over time, as well as the location of the phase curve on one of the branches of a slow surface when projected into a three–dimensional subspace (x_1, x_2, y_2). In the complete system (2), this cycle is formed around a nontrivial point E_1.

Thirdly, the variation y_1 can fall on both the left and right side of the LP point of the bifurcation diagram. As a result, the cycle of the leading system will generate alternating sections of in-phase and anti-phase dynamics in the driven system. An example of this behavior is shown in Fig. 4, *d–f*. During the period of in-phase dynamics, the phase curve lies on the surface of the plane $x_2 = 0$, and during the period of anti-phase — outside this plane (see Fig. 4, *d*), and also partially on the slow surface M^S_{eq} and on an unknown manifold to be found (see fig. 4, *f*). In this case, obviously, there is a hysteresis loop such that an increase or decrease in the value of y_1 leads to the movement of phase points along different equilibriums of the driven system (branches) intersecting at the LP point (see Fig. 4, *d*). When the value of y_1 decreases, there is movement along the line M^0_{eq}, including to the left of the LP point. Then there may be a small surge in numbers prey and predator on the second site, obviously unrelated to bifurcations in the driven system, since it is observed far from the point H. In this case, the trajectory goes to the parabola M^1_{eq}, and the variable y_1 goes to growth until it reaches the LP point. Then it goes back to the straight line M^0_{eq}. In this case, the phase trajectory moves clockwise along the triangle formed by the two branches of the manifold.

In the last two cases, the dynamics in the anti-phase part of the cycle it changes significantly (there is a bursting activity) depending on how close the variation y_1 gets to the point H, as well as on other qualitative changes occurring in the driven system (4). In the examples given above,

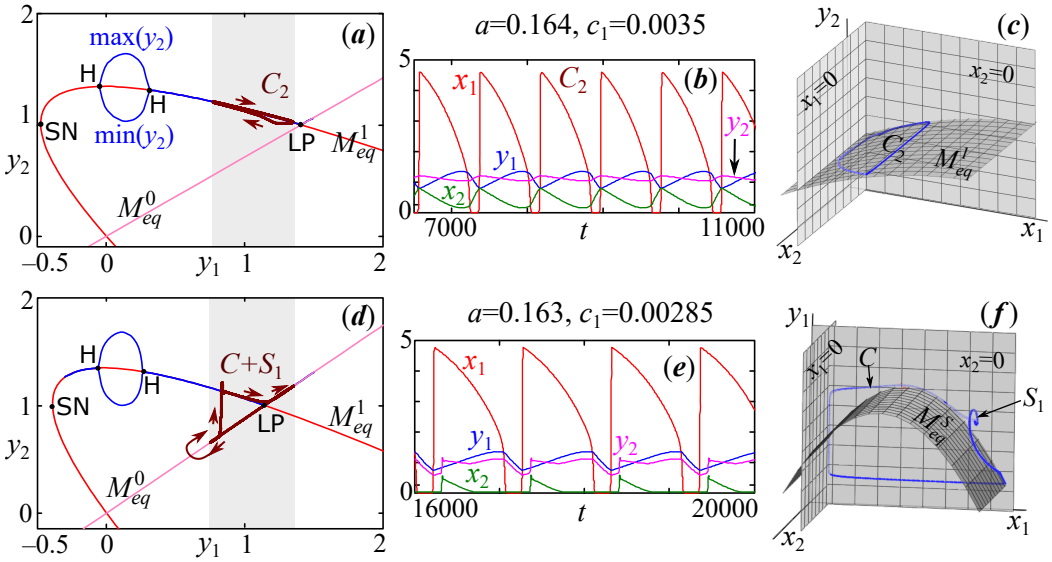

Fig. 4. *a*, *d* — Bifurcation diagrams of system (4) with a change in the parameter y_1 on which the phase points of the periodic solution of system (2) are plotted. *b*, *e* — Examples of dynamics for system (2). *c*, *f* — Location of phase points with respect to critical manifolds (color online)

the limit cycle of the driven system (4) is born (disappears) at two points H lying on a stable branch of stationary states M^1_{eq}. However, with a sufficiently small c_1, the oscillation span in the leading system (3) independently, it never reaches this point. Therefore, with sufficiently small c_1 (parameters from the C area in Fig. 1, *a*) bursting activity based on the driven system cycle can only be part of the transition process if the initial value $y_1(0)$ is located between two points H of the Andronov–Hopf bifurcation (see Fig. 4, *a* or *d*).

When leaving the C region, that is, when increasing c_1, the right point H shifts closer to LP, and so much so that the limit cycle of the leading system captures both the LP point and H. This limit cycle increases its scope so much that the phase points of the system (4) approach an unstable equilibrium and remain in its vicinity for quite a long time. This is indicated by the fact that the middle point of the $\langle y \rangle$ cycle tends to the saddle point. At this moment, the cycle merges with separatrices originating from stationary points and is completely destroyed due to homoclinic bifurcation, marked in Fig. 5 point HB.

In the above diagrams using curves max(y_2) and min(y_2) (see Fig. 5) it is possible to trace how the size of the limit cycle of the driven system (4) changes at different values of the parameters a and c_1. This approach forms the basis of the so-called continuation technique by parameter. The branch of the curve, denoted by $\langle y_2 \rangle$ in Fig. 5, shows the dependence of the average coordinates of the limit cycle. Note that as y_1 decreases, the middle branch of $\langle y_2 \rangle$ approaches to the bottom min(y_2).

Thus, on the upper branch of the stationary states M^1_{eq} of the driven system (4), a limit cycle is formed, which can be considered as the basis of the bursting dynamics of the complete system (2). When the value of y_1 changes, the size and location of the limit cycle of the driven system changes (4). It is easy to understand that in the phase space of the complete system (2), each of these cycles lies on a smooth surface of a parabolic shape originating from the point H. This surface can be considered as an approximation parts of the invariant manifold of the system (2), on which there are rapid bursts of predator and prey numbers (fast manifold). At least, the part of it on which the damped fast periodic movements lie. Denote it by M_{PO}. The presence of this variety makes it possible to immediately explain the mechanism of the birth of triangular

burst shown in Fig. 5, *a*. In the case of such burst, first the trajectory slowly moves down along the line M^0_{eq} (the rest manifold). Then, having reached the minimum value of y_1, the trajectory «jumps» to the fast manifold M_{PO} (to the left of the point H). This jump is accompanied by a rapid growth of the variable x_1. On this manifold, the trajectory makes several turns, corresponding only to damping fluctuations of phase variables. Let's denote this part of the dynamics as S_1. Having reached the point H, the trajectory leaves the fast manifold and ends up on the rest manifold M^1_{eq}. When passing through the LP point the trajectory moves to a line M^0_{eq}, and the cycle closes.

In the second and third examples in Fig. 5, *b*–*c* bursts with a truncated diamond-wave shape arise, which indicates a slightly different mechanism for the formation of fast oscillations and the existence of another branch of a fast manifold. In addition, the transition from the fast manifold M_{PO} to the rest manifold M^1_{eq} occurs significantly to the right of the point H in all cases. In the second example, on a fast manifold, two sections of the dynamics S_1 и S_2 connected by the canard C (see Fig. 5, *b*). The section S_1 consists of damped fast fluctuations at maximum values of $x_1 \gg 0$, S_2 consists of divergent fluctuations at minimum values of $x_1 \approx 0$ (see Fig. 5, *b*).

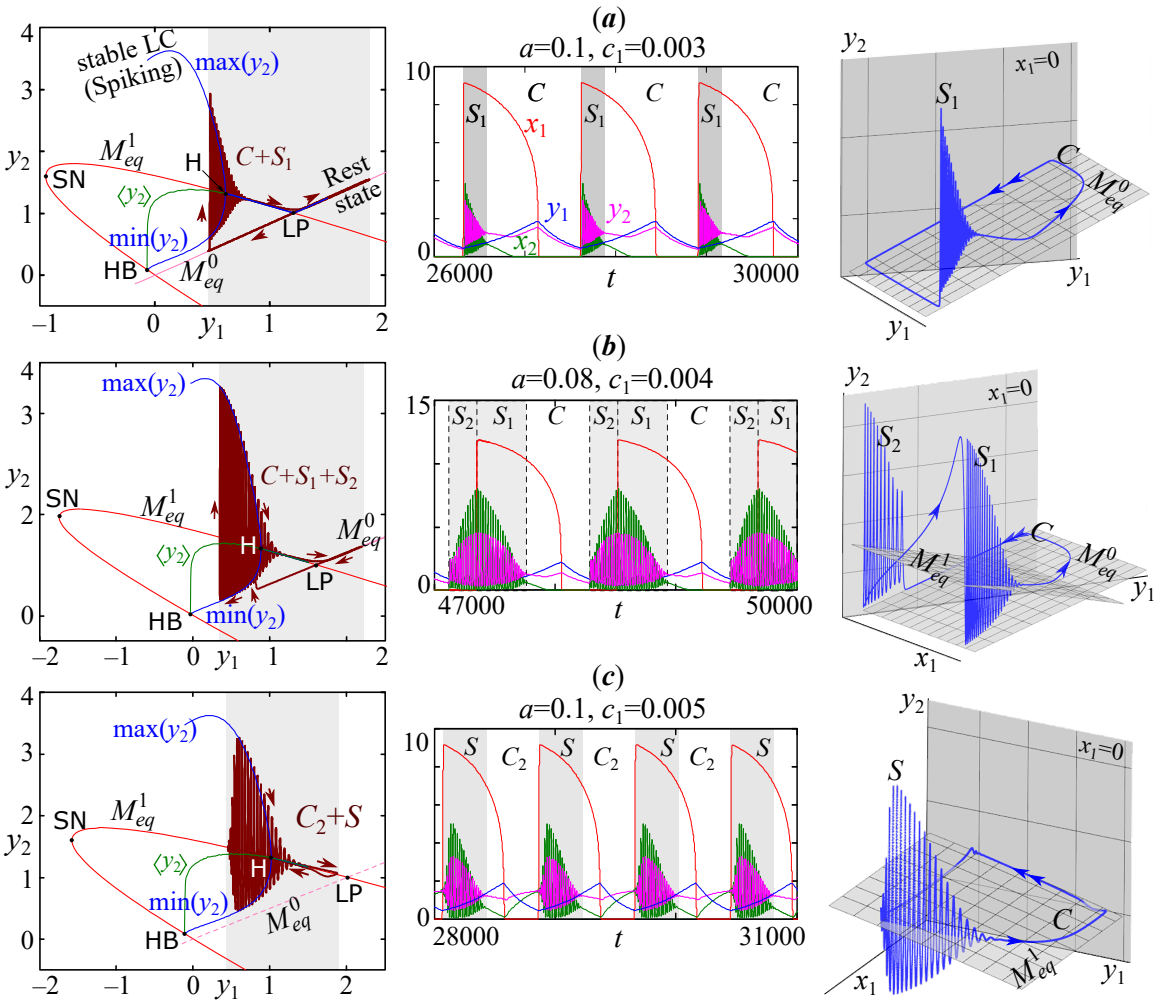

Fig. 5. On the left — the bifurcation diagrams of system (4) with a change in the parameter y_1 and phase points of the periodic solution of system (2). In the middle — examples of the dynamics of system (2). On the right — the view of the attractors and its location relative to the slow manifold (color online)

From this observation, it can be assumed that the birth of rapid explosive oscillations depends not only on the fact of the growth or fall of the y_1 variable of the strong subsystem and its absolute values, but also on the values of the variable x_1. So it is immediately clear that the damped fast fluctuations of S_1 occur only at sufficiently high values of x_1 when the variable y_1 is growing. At low or even close to zero values of x_1, there are no fluctuations or divergent fluctuations of S_2 are born, and the value of y_1 only decreases (see Fig. 5, *b*). From this we can assume that the fast manifold M_{PO} is not the only one, or at least it has an additional branch on which fast divergent oscillations are realized.

This observation was made earlier, in the works [28,30], however, the existence of a second branch of the fast manifold has not been proved there. To verify this statement, we will allocate another subsystem in which the value x_1 is a constant value:

$$\begin{cases} \dfrac{dx_1}{dt} = 0, \\ \dfrac{dy_1}{dt} = c_1\left(-y_1(1+m) + \dfrac{x_1y_1}{1+hx_1} + \dfrac{c_1m}{c_2}y_2\right) = c_1g_1(x_1,y_1,y_2), \\ \dfrac{dx_2}{dt} = x_2(1-ax_2) - \dfrac{x_2y_2}{1+hx_2} = f_2(x_2,y_2), \\ \dfrac{dy_2}{dt} = -c_2y_2 + \dfrac{c_2x_2y_2}{1+hx_2} + c_2m\left(\dfrac{c_2}{c_1}y_1 - y_2\right) = g_2(x_2,y_2,y_1). \end{cases} \tag{5}$$

In the system (5) there is also a small parameter c_1 ($0 < c_1 \ll c_2 < 1$). However, due to the nonlinear dependence of the derivative y_1 on the value of the «frozen» variable x_1, the influence of x_1 on the dynamics and bifurcations of the system (5) should differ significantly from the considered dependencies of the behavior of systems (3) and (4) from the variable y_1.

Let's follow the typical bifurcations of the system (5) at parameter values corresponding to the bursting activity in the system (2) with complex waveforme consisting of a truncated rhombus and a triangle, at $a = 0.11$, $c_1 = 0.0035$ (the other parameters are similar to those used above). In this case, in the complete system (2) there are damped oscillations on the manifold M_{PO}, as well as a series of damped and divergent oscillations on the desired invariant the set M^1_{PO}.

The system (5) has a single nontrivial equilibrium state $E^*(\bar{y}_1, \bar{x}_2, \bar{y}_2)$, which can be found as a solution to a system of equations:

$$\begin{cases} g_1(x_1, \bar{y}_1, \bar{y}_2) = 0, \\ f_2(\bar{x}_2, \bar{y}_2) = 0, \\ g_2(\bar{y}_1, \bar{x}_2, \bar{y}_2) = 0. \end{cases}$$

The nature of the stability of the equilibriums of the system (5) is shown in Fig. 6, *a*, where the solid line corresponds to the dependence of the nontrivial stationary number $\bar{y}_1$ on the value of the parameter x_1, and the dotted line — to the trivial state equilibrium $(0,0,0)$. At the point H^+ there is a supercritical, and at H^-— subcritical bifurcation Andronov–Hopf. To the left of H^+ curve $\bar{y}_1(x_1)$ is approaching to $\bar{y}_1 = 0$ on the positive side, to the right of H^- it is approaching $\bar{y}_1 = 0$ from the negative region. The has a discontinuity at the point $x_1^* = \big(h + 2mh - 1 - m\big)/\big((1-h)(h+2mh-1)\big)$, which together with the points H^+ and H^- can be considered as some threshold values x_1 that determine the type of dynamics. In addition, the system (5) has a semi-trivial equilibrium state $(0, 1/a, 0)$, the coordinate $\bar{y}_1 = 1/a$ of which lies above these lines and is not shown in Fig. 6, *a*. Separatrices originating from a trivial and semi-trivial point generate some regions of attraction of cycles in the system (5).

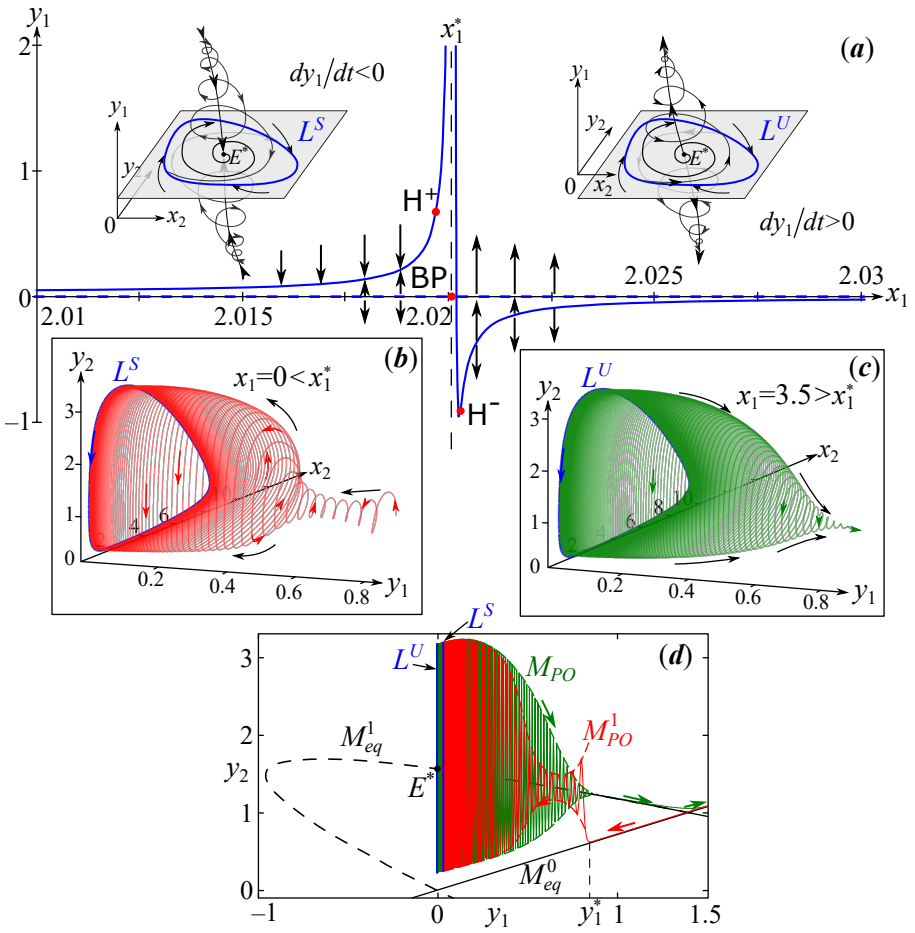

Fig. 6. *a* — Bifurcation diagram at $a = 0.11$, $c_1 = 0.0035$ and phase portraits sketches of system (5). *b* — Transient dynamics of system (5) when moving towards a stable limit cycle L^S and *c* — from an unstable limit cycle L^U. *d* — Approximation of fast manifolds of system (2) by dynamics (cycles) of system (5) (color online)

It is easy to show that to the right of the point x_1^* the derivative is $dy_1/dt > 0$ for any $x_2 > 0$ and $y_2 > 0$, and it does not matter whether they change monotonically or fluctuate. As a result, if $x_1 > x_1^*$, then the variable $y_1(t)$ can only grow indefinitely at $y_1(0) > 0$ (or rather, for the initial conditions above, see Fig. 6, *a*). But since there is a small parameter c_1 in the system (5), the values of y_1 change so slowly that, before leaving the neighborhood of the unstable cycle L^U, the phase the curve makes a large number of turns in its vicinity. The distance between the turns slowly increases as y_1 grows. With time the trajectory contracts to the beam, and all phase variables begin to increase indefinitely and monotonically (Fig. 6, *c*). It can be shown that up to small order $O(c_1)$ this beam coincides with the slow manifold M_{eq}^1 or M_{eq}^0 of the system (4), since these curves coincide with the slow curves of the system (5) at $c_1 = 0$ and are obviously preserved at small disturbance $0 < c_1 \ll 1$.

Fig. 6, *c* shows the dynamics of the system (5) when $x_1 = 3.5$, where the arrows show the directions of the trajectory. It can be seen from the figure that the trajectory is wound on the surface of the parabolic shape M_{PO}, the form of which does not depend on the initial conditions. In this case, it does not matter where to start the integration (outside or inside this figure) or how far from the L^U cycle. The trajectory is quickly attracted to this surface, and then slowly moves along it until it pulls together to the beam M_{eq}^1.

For $x_1 < x_1^*$, the derivative is $dy_1/dt < 0$ for any $x_2 > 0$ and $y_2 > 0$. Therefore, if $x_1 < x_1^*$, then the variable $y_1(t)$ only drops to its stationary value, determined by the dependency $\bar{y}_1(x_1)$. To the right of the point H^+, a stable limit cycle L^S is born, and the variables begin to experience fluctuations. As the value of y_1 decreases slowly enough (due to the small parameter c_1), the phase trajectory is wound onto a surface that has the shape of a one-sheeted hyperboloid, not a paraboloid, as one might expect (fig. 6, *b*). The trajectory transition to this surface occurs as follows. For small $0 < x_1 < x_1^*$, there is some critical value of the variable y_1^* such that for $y_1 > y_1^*$, the variables y_1, x_2 and y_2 fall monotonically enough, and the trajectory of the system (5) moves along M_{eq}^0. When this value is reached and overcome, that is, at $y_1 < y_1^*$, the values of x_2 and y_2 jump in the system (5), which leads to fluctuations. As the values of y_1 fall in the system (5), first there are damped oscillations x_2 and y_2, which under any initial conditions do not reach the curve M_{eq}^1, and then they are replaced by divergent ones. Moving towards a stable limit cycle L^S, the trajectory makes a large number of turns along the surface of M_{PO}^1, the distance between them decreases as it approaches the L^S cycle. Moreover, numerical calculations show that part of the dynamics of the complete system (2), corresponding to damped and divergent oscillations, is sufficient exactly coincides with the two shown in Fig. 6, *d* by system solutions (5). For example, if the starting point of the systems is (5) and (2) lies on the slow manifold M_{eq}^0 at $y_1(0) > y_1^*$ and $x_1 = 0$, then their dynamics will coincide up to small in terms of divergent oscillations by M_{PO}^1 until the transition of the trajectory of the system (2) to the manifold M_{PO}, while the trajectory of the system (5) will continue to move towards the L^S cycle. Similarly for the initial conditions taken on the manifold M_{PO}, the dynamics of (5) and (2) coincide up to small even when switching to branches of a slow manifold M_{eq}^1 and M_{eq}^0.

Thus, the invariant manifolds of the system (5) can be considered as a more accurate approximation of the fast manifold of the system (2) formed by the sections of the trajectory of the system (5) when moving to the limit cycle L^S or the movement from the cycle L^U. They represent two two-dimensional «intersecting» surfaces: a paraboloid M_{PO} and a one-sheeted hyperboloid M_{PO}^1.

For an approximate construction of a parabolic surface M_{PO} (Fig. 7, *b*), it is sufficient to consider several trajectories with starting points from different parts of the unstable cycle L^U and express the coordinates of the phase points in terms of cylindrical coordinates. Then sort the obtained coordinates of the phase points by the growth (or fall) of the value y_1 and interpolate the obtained points, which we will use as a parametrization of the desired surface. In Fig. 6, *c* one of the trajectories used is given. Each additional trajectory it will fill in the gaps in places where the distance between the turns increases. Parameterization of the hyperboloid M_{PO}^1 (Fig. 7, *a*) is performed in a similar way. However, the following values are selected as starting points $y_1(0)$ and $y_2(0)$ on the slow curve M_{eq}^0 ($x_2(0) = 0$), at which the trajectory of the system (5) is as close as possible to the slow curve M_{eq}^1 at the point of transition from damped oscillations to divergent ones. At the same time with this, it is necessary that the transition from monotonous dynamics to fluctuations (a jump from the curve M_{eq}^0 to the surface M_{PO}^1) occurred at the maximum possible value of y_1. Thus , the value is estimated y_1^*.

Fig. 7, *a–c* shows the view of the obtained surfaces. It is easy to notice that the paraboloid M_{PO} intersects the slow curve M_{eq}^1 at its vertex (point H). While for the surface M_{PO}^1 the curve M_{eq}^1 acts as a kind of axis of «symmetry» and does not intersect with it. At the same time, the one-sheeted hyperboloid M_{PO}^1, apparently, concerns the curve M_{eq}^0 at the point y_1^* corresponding to the transition from monotonic dynamics to oscillations in the system (5). In addition, in Fig. 7, *a–c* it is demonstrated that the sections of the system dynamics (2) lie on these surfaces. In this case the trajectory of the complete system (2) is divided into two parts. The first part includes sections of dynamics for which the values of $x_1(t) \approx 0$, in the second part — values of

$x_1(t) \gg 0$. As a result, the first part of the trajectory lies on M^1_{PO} and M^0_{eq} (see fig. 7, *a*). Second — on M_{PO}, M_{eq} and M^0_{eq} (see fig. 7, *b*).

Note that when projecting into other subspaces, the fast manifolds M^1_{PO} and M_{PO} do not intersect as shown in Fig. 7, *c*, and have a slightly different look. In the subspace (x_1, y_1, y_2) M^1_{PO} and M_{PO} — two-dimensional curves that lie on a cylindrical surface with a base of M^S_{eq} and M^U_{eq} ($x_1 > 0$ and $y_2 > 0$) (fig. 7, *e*) forming the framework of the fast-slow cycle in the system (3) (see Fig. 3, *a*). Accordingly, rapid oscillations also lie on this cylinder. In the subspace (x_1, x_2, y_2) M_{PO} is a strongly flattened paraboloid, and M^1_{PO} completely merges with the plane $x_1 = 0$ (Fig. 7, *f*). In both cases, there is a rest manifold between two fast manifolds, along which the trajectory makes a slow movement along the surface of the cylinder with the base M^S_{eq} and M^U_{eq} (see Fig. 7, *e*).

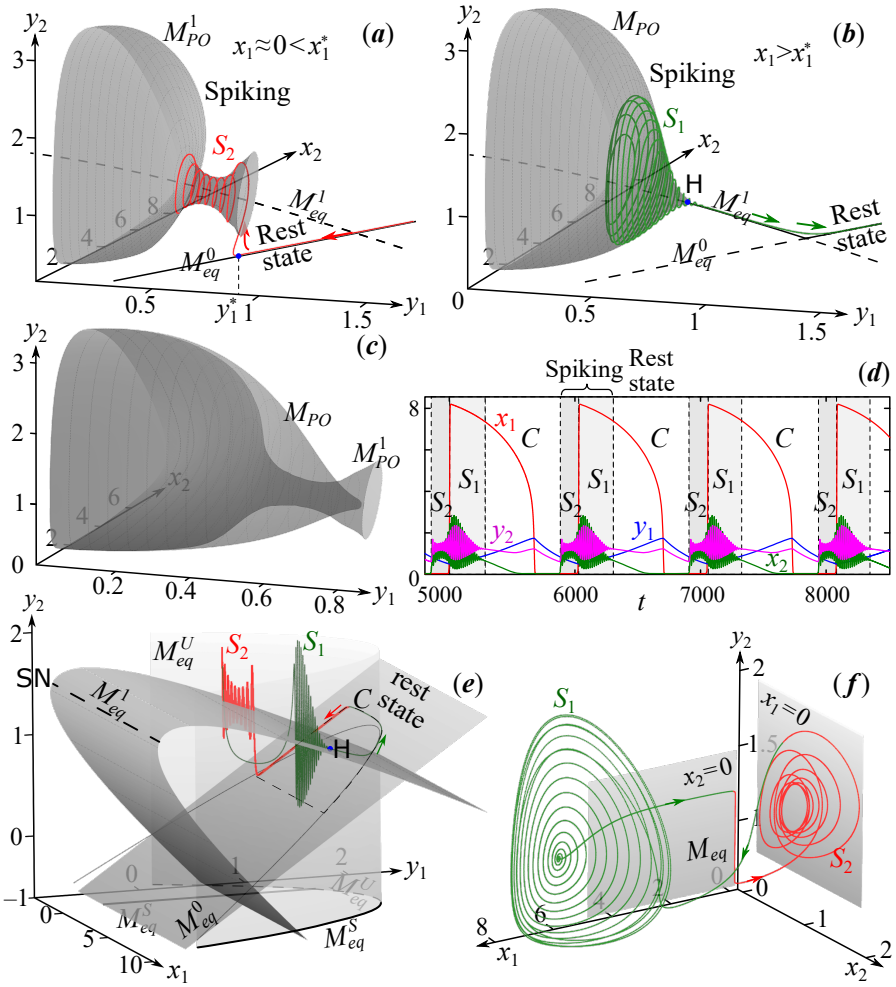

Fig. 7. *a–c* — Two branches of fast manifold M^1_{PO} and M_{PO} on which lie parts of the trajectory of system (2) *a* — with divergent oscillations S_2 ($x_1 \approx 0$) and *b* — with damped oscillations S_1 ($x_1 \gg 0$). *d* — The example of the behavior of system (2) with selected parts of dynamics. *e–f* — Location of the trajectory with respect to slow manifolds M^0_{eq} and M_{eq} (color online)

3. The scenario of the formation of bursts

The presence of different types of activity in subsystems (3), (4) and (5) (monotonous increase or decrease in numbers, as well as damped or divergent oscillations) allows us to describe the scenario of the formation of burst modes of oscillations in the full model (2). This scenario is based on the analysis of the relative position of fast and slow manifolds, as well as on observations of the phase trajectory, which is capable of periodically (or irregularly) jumping between different attractors of the slow and fast subsystem. At first, the phase point moves only along the relaxation cycle (canard) C, corresponding to the phase trajectory of the first (slow) subsystem (3). Then the trajectory is attracted to one of the periodic solutions of the fast subsystem (4) or (5) (for different x_1). In this case, the solutions of the system (2) at $c_1 = 0$ converge to the attractor of the fast subsystem, which is its stable state of equilibrium or limit cycle. When the attractor of a fast subsystem is exponentially stable, then it depends on smooth from y_1. However, smoothness is preserved only at $x_1 \neq x_1^*$. Changing y_1 at some fixed x_1 leads to the formation of a smooth attracting invariant manifold that consists of a slow and a fast part. Let's list them.

- Spatial curves M_{eq}^S and M_{eq}^U, collected from the equilibrium states of a strong community (3), as well as a two-dimensional cylindrical surface based on them.
- Curves formed by the projection of curves M_{eq}^S and M_{eq}^U onto two-dimensional surfaces M_{eq}^0 and M_{eq}^1, which are equilibrium states of a weak community (4) and (5) for $c_1 = 0$.
- A three-dimensional parabolic surface M_{PO} and a one-sheeted hyperboloid M_{PO}^1 (see Fig. 5, *a* and fig. 7), which are formed by cycles of a weak community (5).

The first two parts of the variety correspond to the slow tonic dynamics or rest state of both communities. As shown above, due to the presence of more than one branch, several location options are possible such an attractor (canard) in the phase space. For example, a canard can only lie on the branch M_{eq}^0 (C_1), then the dynamics of predators in both territories will be synchronous, but with zero number of prey in the second community. Or it can only lie on M_{eq}^1 (C_2), then the dynamics will be anti-phase with a non-zero number of prey. Or the canard can be alternately (regularly) located on different branches, then the dynamics of communities will contain periods of synchronous and non-synchronous dynamics that coincide with periods of near-zero ($x_1 \approx 0$) and non-zero ($x_1 \gg 0$) number of prey in the second community (C).

The third part of the variety corresponds to the occurrence of bursting activity or rapid explosive oscillations (spiking) in the second weak community. However, there is the following feature here. Depending on the number of prey in the first territory (x_1), the trajectory leaves the resting state, the subsequent nature of predator dynamics in this territory changes (y_1). If the value of x_1 is high enough, then the value of y_1 obviously it is growing, that is, the predator has enough prey for its development. If x_1 is close to zero, then the value of y_1 can only fall, that is, the predator it dies out in this territory or emigrates.

In the first case ($x_1 \gg 0$), if y_1 is below a certain value (to the left of the point H in Fig. 7, *b*), the trajectory is thrown to the parabolic surface M_{PO}, where it makes several turns. Meaningfully, such dynamic behavior may correspond to the strengthening of competitive relationships between predators of a weak (local individuals) and a strong community (immigrants). As a result, strong competition leads to a rapid population growth in a weak community, which manifests itself in the form of damped fluctuations in the numbers of predators and prey in this territory. These damping fluctuations continue until the number of predators of a strong community grows to a certain value (point H in Fig. 7, *b*). Having reached this value, the trajectory gently returns to a state of rest.

In the second case, when the number of prey of a strong community x_1 is close to zero ($x_1 \approx 0$), the number of predators y_1 falls. If at the same time y_1 reaches a certain value

y_1^*, then the trajectory is abruptly thrown to the hyperboloid M_{PO}^1, on which it is wound. Similarly to the previous case, the competition of immigrants from a strong community with local individuals initiates rapid divergent fluctuations in numbers in a weak community. These fluctuations continue until the minimum possible predator population is reached y_1, in which there is a rapid recovery of prey in a strong community and a slow recovery of predators. In the most extreme case, this happens at the «intersection» of the hyperboloid M_{PO}^1 with the paraboloid M_{PO} in the subspace (y_1, x_2, y_2), that is, at $y_1 \to 0$. After that, the trajectory is rigidly shifted from a hyperboloid to a paraboloid, and the fluctuations are replaced by damped ones against the background of an increase in the number of the predator y_1 of a strong community.

When the system parameters vary (2), both the size of the fast-slow limit cycle and the location of bifurcation points in subsystems change (3), (4) and (5), which act as «edges» of the fast manifold. As a result, different types of bursting activity correspond to different mutual arrangement of the canard and surfaces M_{PO} and M_{PO}^1. Fig. 8 schematically shows the mechanism (scenario) of the formation of different waveform of bursts. To do this, two branches of the fast manifold M_{PO} and M_{PO}^1 they are shown nested in each other and connected by the limiting fast-slow cycle C, and the points where they connect are highlighted with an asterisk.

In Fig. 8, *a* it is shown that if only the fast-slow cycle is asymptotically stable, then the surfaces M_{PO} and M_{PO}^1 exist, but are located away from it. As a result, for parameters from the scope C in Fig. 1, *a*, where in the limiting case in the system (2) only a fast-slow cycle is possible, rapid fluctuations occur under some perturbations of the initial conditions, but as part of the transition dynamics. For example, if we take the starting point in the neighborhood of a fast manifold M_{PO} or M_{PO}^1, then at first the trajectory will make several turns on one of these surfaces, and then it will fall on one of the branches of the slow manifold, where it will make stable periodic movements. This further proves the existence of a fast manifold.

In the case of a triangular-wave bursting, the canard C touches the surface of M_{PO}, and the trajectory begins to move along it independently (Fig. 8, *b*). This happens only after the full recovery of the number of prey of x_1 in a strong community, that is, at $x_1 \gg 0$. In the case of a rhomboid-wave and truncated rhomboid-wave bursting, the canard additionally concerns M_{PO}^1

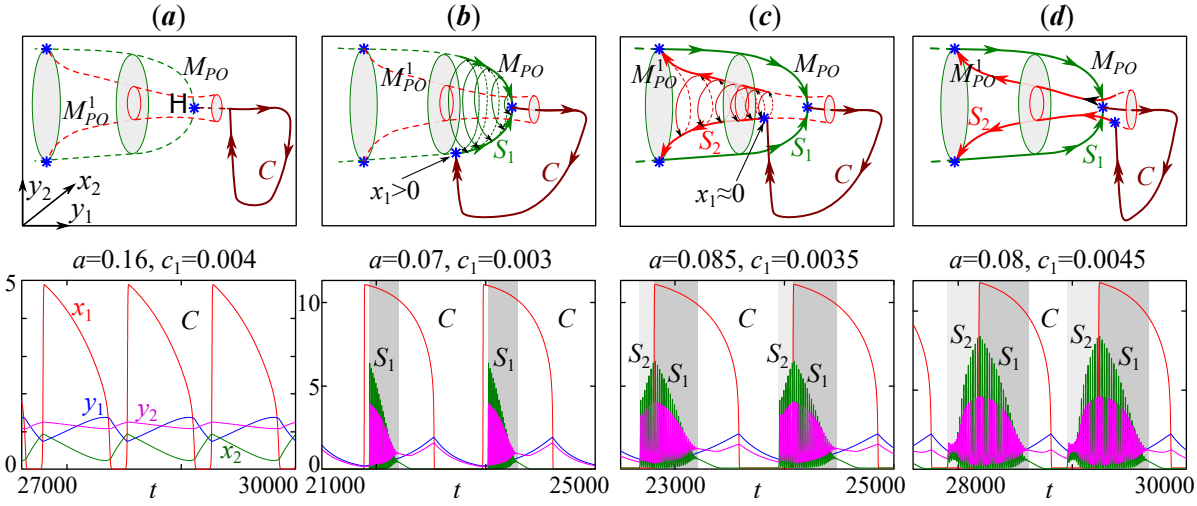

Fig. 8. The first line is the scenario for the formation of various waveforms bursting in the system (2), associated with different positions of the canard C and fast manifolds. The second line is examples of dynamics corresponding to these scenarios: *a* — slow-fast limit cycle (canard), *b* — triangular-wave bursting, *c* — truncated rhomboid-wave bursting and *d* — bursting consisting of a truncated rhombus and a triangle (color online)

(Fig. 8, *c*–*d*), which happens long before the recovery of the number of prey x_1, that is, at $x_1 \approx 0$. But touching a canard with a hyperboloid M^1_{PO} is possible in different places. If the trajectory «intersects» the paraboloid M_{PO}, and then reaches the hyperboloid M^1_{PO}, truncated rhomboid-wave bursting arise (see Fig. 8, *c*). If the trajectory goes to the hyperboloid does not intersect the paraboloid, then a more complex bursting arises, in which the damped oscillations are replaced by divergent, and then again damped (see Fig. 8, *d*). Naturally, there is no intersection of the trajectory and the fast manifold in four-dimensional space. This «intersection» corresponds to a jump in numbers predators y_1 and prey x_1, which is clearly visible when projected into other subspaces (see Fig. 7, *e* и *f*).

Between the last two variants of the arrangement of the canard and the branches of the fast manifold in Fig. 8, *c* and *d* there is an intermediate scenario for the formation of pure diamond-shaped bursting. For example, such as shown in Fig. 5, *c*. In this case, the points where the canard connects to the hyperboloid and then to the paraboloid, they turn out to be as close to each other as possible (the coordinate y_1 coincides). However, being intermediate in location, it occurs in a wide range of parameters. Moreover, it is in this case that it is more often formed quasi-periodic dynamics.

It should be noted that the scenario in Fig. 8 describes the case of completely periodic dynamics, when after each full turn the phase point strictly returns to the same point in the phase space (where the numbers reach exactly the same values), for example, to the point marked with an asterisk. In this case, the time between the appearance of bursting of numbers (the distance between the bursts) turns out to be constant at each full turn of the cycle. In the case of quasi-periodic dynamics (the region Q in Fig. 1) the trajectory on each of its turns returns to a small neighborhood of the starting point. As a result, the connection points of the canard C with one of the branches of the fast manifold form a closed invariant curve. It is not difficult to understand that the surface will be non-orientable, and the trajectory moves along the Klein bottle if the canard is connected to the «inner» the branch M^1_{PO} of the fast manifold (to the left of the point H). If the canard is connected to the «external» branch M_{PO} (to the right of H), then the surface will be orientable, and the trajectory will lie on the torus. In case the parameters fall into one from synchronization tongues (in Fig. 1, *b*), dynamics again it turns out to be periodic, but the trajectory returns to the starting point only after making several full turns on the torus or the Klein bottle.

In general, returning strictly to the same point in the phase space means strict equality of variables at certain intervals. However, for real biological communities, strict equality of numbers is practically unattainable, since random factors constantly shift the phase trajectory away from the stable regime. Therefore, it is more likely that in real communities coupled by migration, functioning according to the described principles and described by the model (2), the time between burst is likely to be unstable, or the dynamics will be quasi-periodic.

Conclusion

When studying the system of two non-identical predator-prey communities coupled by migration, it was found that the leading parameter determining the evolution of bursting activity, and a result, the type of dynamics is the difference in the mortality of predators in different territories. Other parameters, as a rule, determine the stability of the dynamics modes or the shape of the bursts.

With a large difference in the mortality of predators, the considered model refers to to the class of fast-slow systems. The identification of fast and slow variables allowed us to show that the

dynamics in a strong or leading community (a subsystem with low mortality) are long-period fast-slow fluctuations that completely determine the behavior of a weak or driven community (with high mortality). It is shown that, depending on the number of predators of a strong community, the dynamic mode of the driven community smoothly changes: from the slow tonic mode, the weak community gently transitions to rapid burst fluctuations in numbers. However, there is a kind of non-smooth dependence of the dynamics regime of a weak community on the number of prey of a strong one, when with a low or high number of prey of a strong community, the scenario of the birth of rapid fluctuations is different, and the transition between them occurs quite sharply.

Using geometric methods, in the present work it was possible to construct invariant manifolds on which sections with the burst and tonic activity of the system under consideration are realized. As a result, the mechanisms of occurrence of burst with different waveforms were described in detail. The dependence of the shape of fast dynamics on the appearance of an invariant manifold and the location of its parts relative to the fast-slow cycle is discovered and described.

As mentioned earlier, the study of fast-slow systems is a popular area of nonlinear dynamics. In the course of the study of such systems, different dynamics modes are found, the study of which is based on the allocation, as a rule, of only two typical times — fast and slow [18, 20]. The trajectories in this case are formed on the basis of a single fast and slow fast-slow cycle (canard). So, for example, it happens in a three-dimensional modification of the model Rosenzweig-MacArthur, describing the dynamics of systems such as prey-predator-super predator [9]. Qualitatively, such dynamics correspond to the scenario «Fold/Hopf» [17], which is the simplest for the system in question (2). In the slow subsystem (weak community), two bifurcations are observed: saddle-node (fold type) and soft (supercritical) Andronov-Hopf, depending on the value of the «frozen» variable (the number of predators of a strong community). With these two bifurcations, the phase of the bursting dynamics begins and ends. But in most cases (in most of the S area in Fig. 1, *a*) bursting modes are fluctuations of a different type — this is a combination of divergent and damped modes. These two types of fluctuations occur at different values of an additional «frozen» variable (the number of prey of a strong community) and are associated with slow diversity in its different parts. In this case, divergent fluctuations are observed during the recovery of prey on the second territory and, as a rule, precede the restoration of the prey of the first strong community. After that, they are replaced by fading fluctuations and the two communities coexist. In this case, the system obviously has more two typical times. A similar scenario occurs, for example, in some three-dimensional models of neural activity (the Hindmarsh-Rose model) [37, 38]. For them, it was necessary to allocate three different time scales, for each of which its own slow and a fast subsystem, and three layers of slow and fast manifolds nested in each other are described [34, 36, 38].

In this paper, it can be assumed that the damped oscillations in the considered model of coupled communities are the result of soft bifurcation Hopf in a slow-time system, and divergent — hard (subcritical) Hopf bifurcations in a super-slow-time system. Two these cycles end with saddle-node bifurcation of limit cycles or homoclinic bifurcation. In general, the described qualitative rearrangements fit into the scenarios of the formation of burst activity described by E.M. Inzhikevich [17]. However, due to the four-dimensional nature the studied model and the non-smooth dependence on the «frozen» variable (the number of prey of a strong community), new combinations of these scenarios arise, associated with «impossible» for traditional three-dimensional systems ways of connecting trajectories on fast and slow manifolds (through the fourth dimension). In particular, those that «pierce» a fast manifold and generate trajectories on the Klein bottle, or combinations that allow «intersection» of fast manifolds. Such a feature of the dynamics of the community under consideration, without a doubt, requires further detailed

study.

References

1. Frisman YY, Kulakov MP, Revutskaya OL, Zhdanova OL, Neverova GP. The key approaches and review of current researches on dynamics of structured and interacting populations. Computer Research and Modeling. 2019;11(1):119–151 (in Russian). DOI: 10.20537/2076-7633-2019-11-1-119-151.
2. Mukhopadhyay B, Bhattacharyya R. Role of predator switching in an eco-epidemiological model with disease in the prey. Ecological Modelling. 2009;220(7):931–939. DOI: https://doi.org/10.1016/j.ecolmodel.2009.01.016.
3. Saifuddin M, Biswas S, Samanta S, Sarkar S, Chattopadhyay J. Complex dynamics of an eco-epidemiological model with different competition coefficients and weak Allee in the predator. Chaos, Solitons & Fractals. 2016;91:270–285. DOI: 10.1016/j.chaos.2016.06.009.
4. Jansen VAA. The dynamics of two diffusively coupled predator–prey populations. Theoretical Population Biology. 2001;59(2):119–131. DOI: 10.1006/tpbi.2000.1506.
5. Liu Y. The Dynamical Behavior of a Two Patch Predator-Prey Model. Theses, Dissertations, & Master Projects. Williamsburg: College of William and Mary; 2010. 46 p.
6. Saha S, Bairagi N, Dana SK. Chimera states in ecological network under weighted mean-field dispersal of species. Frontiers in Applied Mathematics and Statistics. 2019;5:15. DOI: https://doi.org/10.3389/fams.2019.00015.
7. Shen Y, Hou Z, Xin H. Transition to burst synchronization in coupled neuron networks. Physical Review E. 2008;77(3):031920. DOI: 10.1103/PhysRevE.77.031920.
8. Bakhanova YV, Kazakov AO, Korotkov AG. Spiral chaos in Lotka–Volterra like models. Middle Volga Mathematical Society Journal. 2017;19(2):13–24 (in Russian). DOI: 10.15507/2079-6900.19.201701.013-024.
9. Bakhanova YV, Kazakov AO, Korotkov AG, Levanova TA, Osipov GV. Spiral attractors as the root of a new type of «bursting activity» in the Rosenzweig–MacArthur model. The European Physical Journal Special Topics. 2018;227(7–9):959–970. DOI: 10.1140/epjst/e2018-800025-6.
10. Huang T, Zhang H. Bifurcation, chaos and pattern formation in a space- and time-discrete predator–prey system. Chaos, Solitons & Fractals. 2016;91:92–107. DOI: 10.1016/j.chaos.2016.05.009.
11. Banerjee M, Mukherjee N, Volpert V. Prey-predator model with a nonlocal bistable dynamics of prey. Mathematics. 2018;6(3):41. DOI: 10.3390/math6030041.
12. Yao Y, Song T, Li Z. Bifurcations of a predator–prey system with cooperative hunting and Holling III functional response. Nonlinear Dynamics. 2022;110(1):915–932. DOI: 10.1007/s11071-022-07653-7.
13. Smirnov D. Revealing direction of coupling between neuronal oscillators from time series: Phase dynamics modeling versus partial directed coherence. Chaos: An Interdisciplinary Journal of Nonlinear Science. 2007;17(1):013111. DOI: 10.1063/1.2430639.
14. Dahasert N, Öztürk İ, Kiliç R. Experimental realizations of the HR neuron model with programmable hardware and synchronization applications. Nonlinear Dynamics. 2012;70(4):2343–2358. DOI: 10.1007/s11071-012-0618-5.
15. Wang L, Liu S, Zeng Y. Diversity of firing patterns in a two-compartment model neuron: Using internal time delay as an independent variable. Neural Network World. 2013;23(3):243–254. DOI: 10.14311/NNW.2013.23.015.
16. Santos MS, Protachevicz PR, Iarosz KC, Caldas IL, Viana RL, Borges FS, Ren HP, Szezech Jr JD, Batista AM, Grebogi C. Spike-burst chimera states in an adaptive exponential integrate-and-fire neuronal network. Chaos: An Interdisciplinary Journal of Nonlinear Science.

2019;29(4):043106. DOI: 10.1063/1.5087129.
17. Izhikevich EM. Neural excitability, spiking and bursting. International Journal of Bifurcation and Chaos. 2000;10(6):1171–1266. DOI: 10.1142/S0218127400000840.
18. Han X, Jiang B, Bi Q. Symmetric bursting of focus–focus type in the controlled Lorenz system with two time scales. Physics Letters A. 2009;373(40):3643–3649. DOI: 10.1016/j.physleta.2009.08.020.
19. Gu H, Pan B, Xu J. Bifurcation scenarios of neural firing patterns across two separated chaotic regions as indicated by theoretical and biological experimental models. Abstract and Applied Analysis. 2013;S141:374674. DOI: 10.1155/2013/374674.
20. Chen J, Li X, Hou J, Zuo D. Bursting oscillation and bifurcation mechanism in fractional-order Brusselator with two different time scales. Journal of Vibroengineering. 2017;19(2):1453–1464. DOI: 10.21595/jve.2017.18109.
21. Makeeva AA, Dmitrichev AS, Nekorkin VI. Cycles-canards and torus-canards in a weakly inhomogeneous ensemble of FitzHugh–Nagumo neurons with excitatory synaptic couplings. Izvestiya VUZ. Applied Nonlinear Dynamics. 2020;28(5):524–546 (in Russian). DOI: https://doi.org/10.18500/0869-6632-2020-28-5-524-546.
22. Holling CS. Some characteristics of simple types of predation and parasitism. The Canadian Entomologist. 1959;91(7):385–398. DOI: 10.4039/Ent91385-7.
23. Holling CS. The functional response of predators to prey density and its role in mimicry and population regulation. The Memoirs of the Entomological Society of Canada. 1965;97(S45):5–60. DOI: 10.4039/entm9745fv.
24. Bazykin AD. Mathematical Biophysics of Interacting Populations. Moscow: Nauka; 1985. 181 p. (in Russian).
25. Bazykin AD. Nonlinear Dynamics of Interacting Populations. World Scientific Series on Nonlinear Science Series A: Vol. 11. New–Jersey, London, Hong Kong: World Scientific; 1998. 216 p. DOI: 10.1142/2284.
26. Rosenzweig ML, MacArthur RH. Graphical representation and stability conditions of predator–prey interactions. The American Naturalist. 1963;97(895):209–223. DOI: 10.1086/282272.
27. Rinaldi S, Muratori S. Slow-fast limit cycles in predator-prey models. Ecological Modelling. 1992;61(3–4):287–308. DOI: 10.1016/0304-3800(92)90023-8.
28. Kulakov MP, Kurilova EV, Frisman EY. Synchronization and bursting activity in the model for two predator–prey systems coupled by predator migration. Mathematical Biology and Bioinformatics. 2019;14(2):588–611 (in Russian). DOI: 10.17537/2019.14.588.
29. Kurilova EV, Kulakov MP, Frisman EY. Effects of synchronization by fluctuations in numbers of two predator–prey communities at saturation predator growth and limitation of the prey number. Information Science and Control Systems. 2015;(3(45)):24–34 (in Russian).
30. Kurilova EV, Kulakov MP. Quasi-periodic dynamics in a model of predator–prey communities coupled by migration. Regional Problems. 2020;23(2):3–11 (in Russian). DOI: 10.31433/2618-9593-2020-23-2-3-11.
31. Dhooge A, Govaerts W, Kuznetsov YA, Meijer HGE, Sautois B. New features of the software MatCont for bifurcation analysis of dynamical systems. Mathematical and Computer Modelling of Dynamical Systems. 2008;14(2):147–175. DOI: 10.1080/13873950701742754.
32. Benoît E, Callot JL, Diener F, Diener M. Chasse au canard. Collectanea Mathematica. 1981;31–32:37–119 (in French).
33. Arnold VI, Afraimovich VS, Ilyashenko YS, Shilnikov LP. Bifurcation theory and catastrophe theory. In: Dynamical Systems V. Vol. 5 of Encyclopaedia of Mathematical Sciences. Berlin: Springer-Verlag; 1994. P. 1–205.

34. Ersöz EK, Desroches M, Mirasso CR, Rodrigues S. Anticipation via canards in excitable systems. Chaos: An Interdisciplinary Journal of Nonlinear Science. 2019;29(1):013111. DOI: 10.1063/1.5050018.
35. Shilnikov A, Cymbalyuk G. Homoclinic bifurcations of periodic orbits on a route from tonic spiking to bursting in neuron models. Regular and Chaotic Dynamics. 2004;9(3):281–297. DOI: 10.1070/RD2004v009n03ABEH000281.
36. Kolomiets ML, Shilnikov AL. Qualitative methods for case study of the Hindmarch–Rose model. Russian Journal of Nonlinear Dynamics. 2010;6(1):23–52 (in Russian). DOI: 10.20537/nd1001003.
37. Hindmarsh JL, Rose RM. A model of neuronal bursting using three coupled first order differential equations. Proc. R. Soc. Lond. B. 1984;221(1222):87–102. DOI: 10.1098/rspb.1984.0024.
38. Linaro D, Champneys A, Desroches M, Storace M. Codimension-two homoclinic bifurcations underlying spike adding in the Hindmarsh–Rose burster. SIAM Journal on Applied Dynamical Systems. 2012;11(3):939–962. DOI: 10.1137/110848931.